Normal-fluid velocity measurement and superfluid vortex detection in thermal counterflow turbulence

Demosthenes Kivotides
Department of Chemical Engineering, University of California, Santa Barbara, California 93117, USA
(Received 16 October 2008; published 1 December 2008)

A first-principles analysis, which self-consistently takes into account the collisions of tracer particles with quantum vortices, demonstrates that there exist feasible thermal counterflow turbulence particle image velocimetry experiments that, for sustained periods of time, very accurately record the normal-fluid velocity. Moreover, sporadic, abrupt, and readily discernible deviations of tracer particle velocity from normal-fluid velocity always correspond to nonarresting particle-vortex collisions of finite duration that do not nullify the experiment and allow unambiguous pointwise-accurate tracking of quantum vortex position.

DOI: 10.1103/PhysRevB.78.224501 PACS number(s): 67.25.dk, 47.37.+q, 47.55.Iv

Thermal superfluids[1–3] hold a special position within quantum physics. Indeed, they allow accessible laboratory tests of basic quantum field-theoretic ideas and exhibit the important phenomenon of Bose-Einstein condensation. Because of the latter, there exists a nontrivial ground state that corresponds to the superfluid component while the thermal quasiparticle excitations of this ground state correspond to the normal-fluid component. The superfluid component dynamics is described by nonlinear generalizations of the Schrödinger equation, predicting accordingly the existence of quantized vortices. Despite the conceptual and practical importance of both superfluid vortices and normal-fluid flow, it has been proven difficult until now to directly measure the local normal-fluid velocity and unambiguously track, with pointwise accuracy, dynamical individual quantum vortex positions. Indeed, Zhang and Van Sciver[4] released micron-sized solid particles in thermal counterflow turbulence and found that their recorded velocities do not correspond to the velocity of the normal fluid. On the other hand, Bewley *et al.*[5] employed tracer particles in order to visualize superfluid vortices assuming that, following a collision, the former are trapped by the latter. Kivotides and co-workers[6–8] analyzed this hypothesis and concluded that it is not generally valid, thus requiring careful qualification in every particular case. Recently, the particle image velocimetry (PIV) experiment of Zhang and Van Sciver[4] was also analyzed by Kivotides[9] who clarified the underlying physical processes and obtained excellent agreement between measurements and first-principles computations that take into account, in a self-consistent fashion, particle-vortex collisions. The key theoretical findings are: (a) away from an isolated superfluid vortex, viscous drag causes a particle to move with the normal-fluid velocity,[10] (b) when a particle collides with a straight superfluid vortex at finite temperature, there is a critical approaching velocity below which the particle is trapped by the vortex,[6,7] and (c) for high normal-fluid counterflow velocities, the developed turbulent tangle in the superfluid is so dense that, although a particle escapes its collisions with the vortices, the effect of the latter on its motion is so large that any possibility for normal-fluid velocity measurement is lost.[9] These findings bring forward the following riddle: Are counterflow turbulence experiments in which the normal-fluid velocity is large enough to be above the trapping critical velocity threshold but at the same time small enough not to create dense counterflow tangles (which by interacting with particles eliminate any possibilities for local normal-fluid measurement) allowed by the dynamical laws of superfluid physics? In this contribution, we analyze this enigma from first principles and show that it has a positive resolution. Thus, we propose a feasible PIV thermal counterflow turbulence experiment that, despite sporadic particle collisions with superfluid vortices, does not involve particle trapping and accurately registers for sustained periods of time the local normal-fluid velocity. Moreover, in this experiment, a particle that, for a finite period of time between collision and detachment instants, fails to record the normal-fluid velocity not only does not manifest experimental failure but, instead, unambiguously tracks the motion of the quantum vortex that during this period is attached to it. The definiteness of vortex tracking is due to the fact that particle-vortex collisions cause abrupt and intense particle-velocity oscillations that cannot be confused with the much smoother normal-fluid velocity time series. The harmonious combination of these two features ensures that future PIV experiments, of the type outlined here, could play a decisive role in probing essential superfluid physics.

The mathematical model includes, in a self-consistent fashion, particle-vortex collision physics. In particular, denoting by $\mathbf{X}(\ell,t)$ the superfluid vortex tangle $\mathcal{L}$, where ℓ is the arclength parametrization along the vortices and t is time, the superfluid vortex dynamics obeys the following law:

$$\frac{\partial \mathbf{X}}{\partial t} = \mathbf{V}^s + \mathbf{V}^b + \mathbf{V}^\phi + \mathbf{V}^f. \tag{1}$$

The first contribution to the right-hand side is the vortex-induced superfluid velocity $\mathbf{V}^s$ that is given by the Biot-Savart integral,

$$\mathbf{V}^s(\mathbf{x}) = -\frac{\kappa}{4\pi}\int_{\mathcal{L}} d\ell \frac{\mathbf{X}' \times (\mathbf{X}-\mathbf{x})}{|\mathbf{X}-\mathbf{x}|^3}, \tag{2}$$

where $\mathbf{X}' \equiv \partial \mathbf{X}/\partial \ell$ is the unit tangent vector (along the direction of the singular superfluid vorticity) and κ is the quantum of circulation. The distortion of vortex-induced flow by a particle immersed in the fluid is taken into account by the $\mathbf{V}^b$ term.[11] Notably, the model departs from traditional point-

particle treatments of classical multiphase fluids[12] by depicting suspended particles as finite spheres and satisfying explicitly the solid-liquid interface boundary condition which requires the fluid velocity to be along the tangent of the particle surface. This approach, as well as the application of numerical and computational vortex methods to superfluids, was pioneered by Schwarz.[13,14] In these works however, the vortices collided with fixed particles while here the collision dynamics are treated self-consistently.[6,7] The superflow velocity field $\mathbf{V}^{\phi}$ corresponds to the motion of a spherical particle with velocity $\mathbf{V}^{p}$ in a uniform unbounded inviscid flow with velocity $\mathbf{V}^{s,c}$. The latter is the superfluid counterflow velocity that, together with the normal-fluid counterflow velocity, satisfies mass conservation $\rho_s \mathbf{V}^{s,c} + \rho_n \mathbf{V}^{n,c} = 0$. Here, ρ_s is the superfluid mass density and ρ_n is the normal-fluid mass density. $\mathbf{V}^{\phi}$ is given by[6]

$$\mathbf{V}^{\phi}(\mathbf{x}|\mathbf{z}) = \mathbf{V}^{s,c}(\mathbf{x}) + 0.5\left(\frac{a}{r}\right)^3 [\mathbf{V}^{s,c}(\mathbf{z}) - \mathbf{V}^{p}(\mathbf{z})] \cdot \left(\mathbf{I} - 3\frac{\mathbf{x}'\mathbf{x}'}{r^2}\right), \tag{3}$$

where $\mathbf{V}^{\phi}(\mathbf{x}|\mathbf{z})$ is the velocity of the superfluid at $\mathbf{x}$ when the center of a sphere of radius a is located at $\mathbf{z}$, $\mathbf{I}$ is the 3×3 unit matrix, $\mathbf{x}' = \mathbf{x} - \mathbf{z}$, and $r = |\mathbf{x} - \mathbf{z}|$. $\mathbf{V}^{f}$ models mutual friction effects on the vortices[15]

$$\mathbf{V}^{f} = h_{\star}\mathbf{X}' \times [\mathbf{V}^{n,c} - (\mathbf{V}^{s} + \mathbf{V}^{b} + \mathbf{V}^{\phi})] + h_{\star\star}[\mathbf{X}' \times (\mathbf{X}' \times \mathbf{V}^{n,c}) + \mathbf{V}^{s} + \mathbf{V}^{b} + \mathbf{V}^{\phi}], \tag{4}$$

where $\mathbf{V}^{n,c}$ is the kinematically prescribed counterflow normal-fluid velocity and $h_{\star}$, $h_{\star\star}$ are dimensionless mutual friction coefficients.[6,15] The particle equation of motion[9] extends the Schwarz equation of motion[13] (which refers to a particle in a pure superfluid) to the realm of thermal superfluids by taking into account normal-fluid effects on the particle,

$$m_e \frac{d\mathbf{V}^{\mathbf{p}}}{dt} = 6\pi a \mu_n (\mathbf{V}^{n} - \mathbf{V}^{p}) + 2\pi\rho_s a^3 \frac{\partial \mathbf{V}^{s}(\mathbf{z},t)}{\partial t} + \frac{1}{2}\rho_s \int_S dS (\mathbf{V}^{s} + \mathbf{V}^{b})^2 \hat{\mathbf{n}}, \tag{5}$$

where m_e is the effective particle mass $m_e = m + (2/3)\pi(\rho_s + \rho_n)a^3$, m is the particle mass, μ_n is the dynamic viscosity of the normal fluid, and $\mathbf{V}^{s}(\mathbf{z},t)$ is the vortex-induced velocity at the particle center. The particle is neutrally buoyant. A few remarks about the plausibility of the proposed mathematical model are appropriate here. First, how important is the lack of self-consistent treatment for the normal-fluid? Although a replacement of the kinematic normal-fluid modeling by a dynamical one is a desirable future development, Kivotides[9] obtained very good agreement between the present model and the Zhang-Van Sciver[4] measurements. Noting moreover that the analysis of Kivotides[9] referred to the motion of a particle in very dense tangles with corresponding dynamical complexity (due to multiple simultaneous particle-vortex collisions), far greater than the complexity of the cases studied here, we have every reason to trust the adequacy of our model. In addition, the important normal-fluid effects on the particle are modeled by a drag force of viscous origin (due to normal-fluid flow around the particle known as Stokes flow) and an "added mass force" that takes into account the work that the particle has to do on the fluid when it accelerates through it. In order to take advantage of the rich and complex physics of the model, we ought to employ accurate methods for its solution. We apply the methods developed by Kivotides *et al.*[6] Kivotides *et al.*[6] demonstrated in great detail the accuracy of the solid-liquid interface treatment. The accuracy of our vortex dynamics methods was demonstrated by Kivotides and Wilkin.[8]

The working superfluid is 4He. We performed a trial and error procedure with various counterflow velocities, temperatures, and system sizes in order to find a set of flow parameters that answers the riddle posed in the introduction. The suggested values were $V_y^{n,c} = -10$ cm s^{-1} for the normal-fluid counterflow velocity along the y direction, $T = 1.3$ K for the temperature, and $l_b = 0.005$ cm for the system size. The solid-liquid interface boundary condition which requires the fluid velocity to be along the tangent of the particle surface is enforced in all computations with at least 0.1° of accuracy, and the number of terms in the Legendre expansion in the computation of $\mathbf{V}^{b}$ (Refs. 11 and 13) required for this accuracy does not exceed 30. The tracer particle radius is $a = 10^{-4}$ cm and is resolved with at least six vortex segments. This resolution has been proven adequate[9] in depicting smooth vortex contour dynamics at the scale of the particle size and results in discretization length $\delta l \approx 1.56 \times 10^{-5}$ cm along the vortices. The typical time step is $\delta t \approx 0.3 \times 10^{-7}$ s. This time step resolves both the fastest Kelvin waves in the system and viscous effects on the particle since it is always smaller than 0.1τ, where τ is the Stokes time $\tau = a^2\rho_p / 3\mu_n$. We first establish a steady-state counterflow turbulence in the absence of any particles. For the aforesaid choices of normal-fluid counterflow velocity, temperature, and system size, we find a steady-state vortex line density equal to $\lambda = 0.1168 \times 10^7$ cm^{-2}. The particle is then inserted as described in Ref. 9 with zero initial velocity at distance of $1.6a$ from the boundary of the computational domain. The calculations stop when the particle reaches the end of the box.

We have performed 11 computations (with random initial particle positions on the x-z plane) in order to draw generally valid inferences. A sample initial condition is shown in Fig. 1 (top). The results support a number of conclusions. First, in 6 out of 11 cases, the particle propagates throughout the box without a single collision with vortices. In these cases, the particle velocity is approximately equal to the normal-fluid velocity. A typical time series is shown in Fig. 1 (bottom). Notably, there is an initial transient during which the particle's velocity adjusts (because of drag forces) to the normal-fluid velocity. Defining the particle response time as the time needed for its velocity to grow to 63% [i.e., $(e-1)/e$] of the normal-fluid velocity, we find a numerical response time $t_r = 3.057 \times 10^{-5}$ s. Therefore, since $\tau = 3.193 \times 10^{-5}$ s, viscous effects are accurately captured. These data constitute proof that highly accurate normal-fluid velocity measurement for sustained periods of time is possible in superfluids. Certainly, this was first pointed out in Ref. 10, where the particle was idealized as a point. However, as discussed in

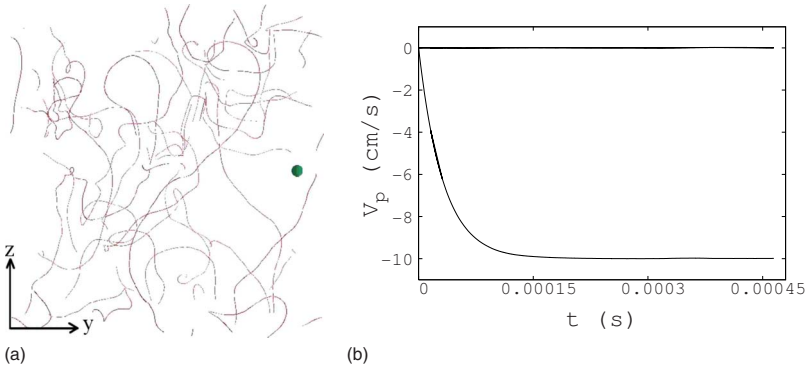

FIG. 1. (Color online) (a) Sample initial configurations for particle and vortex tangles in a thermal counterflow at temperature $T=1.3$ K and normal-fluid velocity $V_y^{n,c}=-10$ cm s^{-1}. The particle has initial velocity zero. (b) Particle-velocity components versus time for a typical evolution without collisions. Evidently, the particle tracks the normal-fluid velocity with great accuracy. Also observed is the initial response-time regime.

Ref. 8 and in opposition to the classical fluids case, a point-like particle is a drastic approximation in the context of quantum fluids. Equally important, Ref. 10 dealt with a single vortex ring and not a turbulent tangle. Thus, the new element here is that, despite finite particle size and vortex tangle complexity, the tangle is dilute enough for nonattached vortices to have a negligible effect on particle motion. Definitely, there are instances when a vortex approaches a particle close enough to induce a deviation of the latter's velocity from the normal-fluid one but the results show that

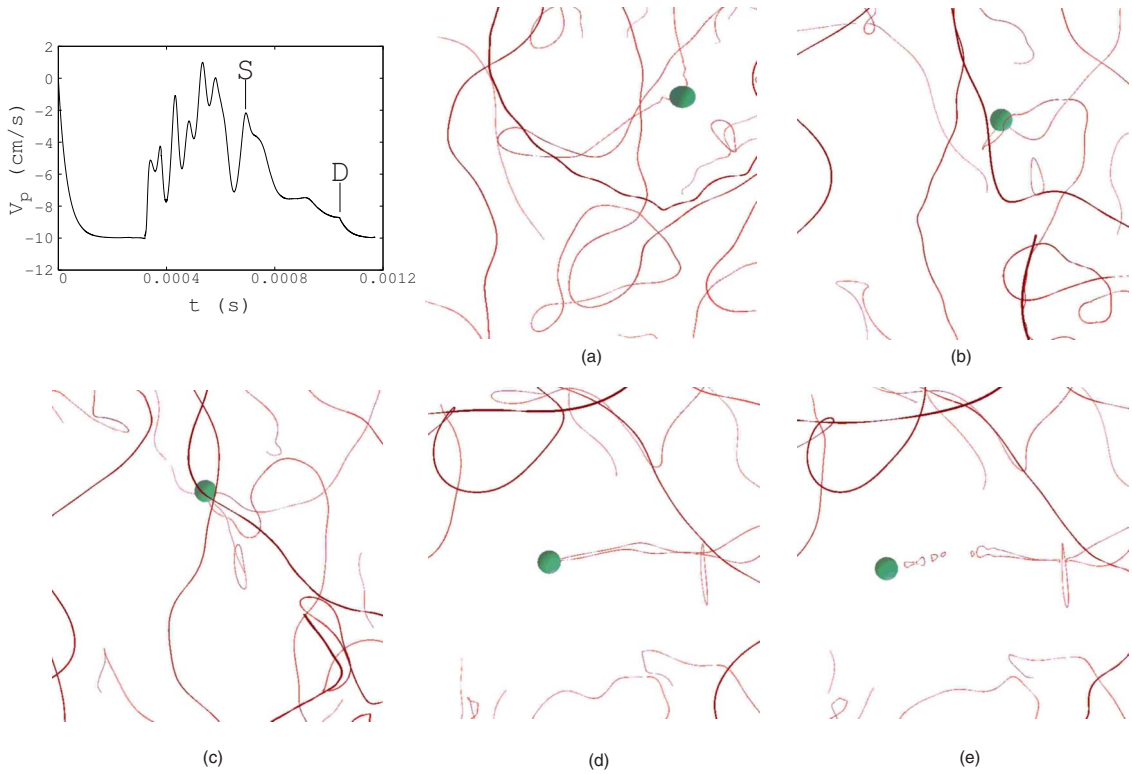

FIG. 2. (Color online) On the upper left: particle-velocity time series for the longest particle-vortex collision. (a) The collision point is fixed by the onset of strong oscillations ($t_a=3.23\times10^{-4}$ s), where the generation of Kelvin waves is also observed. Following the collision is the odographic-vortex regime of particle travel (b) along the vortex ($t_b=6.33\times10^{-4}$ s), which is characterized by strong high-frequency particle-velocity oscillations and (c) ends at point S ($t_c=7.0\times10^{-4}$ s). Subsequently, the regime of particle induced vortex stretching starts. The dynamics here leads to the formation of a characteristic (d) protruding spike ($t_d=9.95\times10^{-4}$ s) and corresponds to a nonoscillatory tendency of the particle's velocity to equalize itself with the normal-fluid velocity. This regime ends at (e) point D ($t_e=10.40\times10^{-4}$ s) where the vortex detaches from the particle via a sequence of reconnections that take place once the aforesaid vortex spike becomes too narrow. Finally, the particle, free of vortices, recovers (due to viscous drag) the normal-fluid velocity. The formation of such pronounced long spikes is not a universal feature of particle-vortex detachment processes since it depends on the degree of vortex-outline alignment with the counterflow direction in the neighborhood of the collision site.

such deviations are at most 4% of the normal-fluid velocity and do not contaminate significantly the measurement. This 4% magnitude also indicates that normal-fluid fluctuations caused by mutual friction excitation from the superfluid vortices are not problematic in the context of the present conclusions since, as shown by Kivotides,[16] their corresponding Reynolds number is smaller than unity while the present normal-fluid Reynolds number is Re=21.4558. Therefore, their magnitude is comparable to the strongest fluctuations induced on particle velocity by the totality of the nonattached vortices. In the other cases, the particle collides with the tangle. Does this nullify a PIV experiment? Our analysis suggests that the phenomenology of such collisions is governed by simple laws that answer this question negatively. Most importantly, collisions are readily discernible (in the particle's velocity time series) events that never result in particle-vortex locking or sustained particle-motion reversals. Moreover, the post-collisional particle behavior depends upon the relative orientation of the vortex contour in the vicinity of the collision site with respect to the counterflow direction. In particular, when the vortex outline opposes or extends normally to the counterflow direction, the particle is first acted upon by a strong decelerating collision-induced force before continuing its forward motion dragging the vortex behind it, always breaking free eventually. If, however, the vortex outline aligns (to a greater or lesser degree) with the counterflow direction, the particle, without altering the direction of its motion, travels along it while at the same time suffering rapid high-frequency velocity vibrations that strongly differ from the precollisional normal-fluid tracking regime time series. This "odographic-vortex" regime lasts until the particle has to choose between following further the vortex contour against the counterflow and escaping. For the particular flow conditions here, the particle always chooses the second option, and after dragging the vortex behind it forming a characteristic protruding spike configuration, it finally separates from it. This dragging regime is also discernible in an experiment. First, it differs from the odographic-vortex regime by the much smoother oscillation-free particle-velocity time series that characterize it and from the postdetachment viscous-drag-dominated regime by the much less pronounced (although still monotonic) tendency of particle velocity to equalize itself with the normal-fluid velocity. This latter feature is associated with the pull of the trailing vortex. Notably, in all computations performed here, breakaway particles do not carry any attached small rings despite the fact that such cases cannot be excluded in principle. The conclusions are exemplified in the context of the longest particle-vortex collision computed here, as shown in Fig. 2. The duration of this collision was $\Delta t = 6.8 \times 10^{-4}$ s. For comparison, in the shortest collision case, $\Delta t = 1.3 \times 10^{-4}$ s.

In conclusion, the impact of the present results on PIV experiments is positive since they rigorously show that there is a range of counterflow turbulence parameters within which an interpretation of measurements in terms of an unambiguous sequence of highly accurate normal-fluid velocity and superfluid vortex contour tracking regimes is possible. It is also important to note that, in case of a turbulent normal fluid in homogeneous systems, things are not so straightforward. Particle-velocity fluctuations induced by collisions with vortices would introduce high-frequency particle-velocity fluctuations that could be confused with genuine turbulent normal-fluid fluctuations. Moreover, the governing dynamical laws do not support a fully developed turbulent normal fluid coexisting with a dilute vortex tangle. Dynamically consistent tangles would be dense and, via frequent collisions with particles, would decorrelate the velocity of the latter from the velocity of the normal fluid.

[1] R. J. Donnelly, *Quantised Vortices in Helium II* (Cambridge University Press, Cambridge, 1991).
[2] W. F. Vinen and J. J. Niemela, J. Low Temp. Phys. **128**, 167 (2002).
[3] A. P. Finne, V. B. Eltsov, R. Hanninen, N. B. Kopnin, J. Kopu, M. Krusius, M. Tsubota, and G. E. Volovik, Rep. Prog. Phys. **69**, 3157 (2006).
[4] T. Zhang and S. W. Van Sciver, J. Low Temp. Phys. **138**, 865 (2005).
[5] G. P. Bewley, D. P. Lathrop, and K. R. Sreenivasan, Nature (London) **441**, 588 (2006).
[6] D. Kivotides, C. F. Barenghi, and Y. A. Sergeev, Phys. Rev. B **77**, 014527 (2008).
[7] D. Kivotides, C. F. Barenghi, and Y. A. Sergeev, Phys. Rev. B **75**, 212502 (2007).
[8] D. Kivotides and S. L. Wilkin, J. Fluid Mech. **605**, 367 (2008).
[9] D. Kivotides, Phys. Rev. B **77**, 174508 (2008).
[10] D. Kivotides, C. F. Barenghi, and Y. A. Sergeev, Phys. Rev. Lett. **95**, 215302 (2005).
[11] D. Kivotides, C. F. Barenghi, and Y. A. Sergeev, J. Low Temp. Phys. **144**, 121 (2006).
[12] D. Kivotides, C. F. Barenghi, A. J. Mee, and Y. A. Sergeev, Phys. Rev. Lett. **99**, 074501 (2007).
[13] K. W. Schwarz, Phys. Rev. A **10**, 2306 (1974).
[14] K. W. Schwarz, Phys. Rev. B **31**, 5782 (1985).
[15] D. Kivotides, Phys. Rev. B **76**, 054503 (2007).
[16] D. Kivotides, Phys. Lett. A **341**, 193 (2005).